High Accuracy Measurement Technology of CCD and its Industrial Application

Pengfei Hao, Xiaodong Zhang and Yuanzong Li
College of Mechanical Engineering
Taiyuan University of Technology
Taiyuan, Shanxi030024, China
bianyuanganqingjita@sina.com

Lihong Zheng
Faculty of Information Technology
University of Technology
NSW 2007, Sydney, Australia
lzheng@it.uts.edu.au

***Abstract*—This paper introduces a subpixel measuring method for industry dimension measurement. The new point is high accurate edge point location which is to use spatial moments to estimate the exact location of edge within a pixel. The proposed method includes of camera calibration, image preprocessing, edge detection, subpixel location and dimension obtain. In practical, there are many factors which affect the measurement result. Noise may play key role. In order to eliminate the noise effect on measurement, meanwhile, to keep it from expanding and save the details of image edge, a nonlinear filter algorithm is proposed. Furthermore, subdivision technology based on spatial moment help to improve accuracy of edge location. Real time industrial measure results have demonstrated that high accuracy dimensional measurement technology could reach the accuracy index whose maximum measure error less than 0.01 mm. Therefore, this new method can be further developed and applied in many kinds of real time applications.**

***Keywords*—industrial measurement, subpixel, calibration of camera**

I. INTRODUCTION

Since a charge-coupled device (CCD) invented by Bell laboratory of America in 1969 digital photograph technology [1] has been developed at faster speed. There are many successful applications such as note dimension measurement technology [2], measurement of internal thread of ball screws [3] and so on. Within these applications high accuracy dimension measure has become more and more important for cutting cost and increasing company's revenue.

Measurement technology based on camera is not a new area and many traditional image processing technology such as the filter, edge detection, the spatial moment and the subdivision technology are applied in industrial measuring system. Our method, compared with other existing methods, such as note dimension measurement technology, has many advantages. First of all, this method is untouched, which is suitable for measuring some flimsy and crisp pieces [4]; Secondly, it is fast due to all process can be finished within 10 milliseconds; Lastly, it is high accurate because the measure accuracy is with μm [5]. Therefore, this new method can be further developed and applied in many kinds of real time applications.

II. IMAGE PROCESSING AND EDGE DETECTION

A. Principle of Camera Calibration

Camera calibration [6] is to find the relationship between CCD plane and measuring plane. By analysis of a standard piece whose parameter, such as size, are known exactly, coefficient S, which stands for length of each pixel, can be gotten. Therefore, the size of work piece can be obtained. Following is explained in detail.

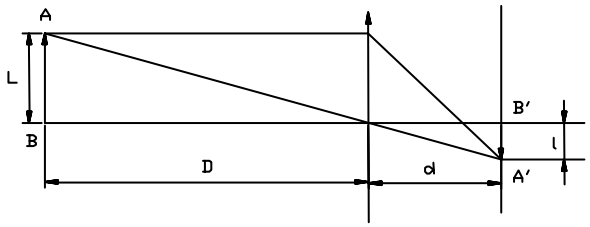

Fig. 1 Diagram of camera calibration principle

In Figure 1 *A'B'* is image of object *AB* in CCD array plane, the length of *AB* is *L* while the length of *A'B'* is *l*, the distance from *AB* to lens is D, another distance from *A'B'* to lens is *d*, calibration coefficient *S* is calculated when both *l* in pixel unit and *L* of standard piece are known.

$$\text{As} \quad \frac{l}{L} = \frac{d}{D} \tag{1}$$

$$\text{So} \quad l = \frac{d}{D} L \tag{2}$$

Transfer coefficient *S* is denoted by,

$$S = \frac{L}{l} = \frac{L}{d/D\,L} = \frac{D}{d} \tag{3}$$

Therefore, the size of objects can be given by,

$$L = S \cdot l \tag{4}$$

Considering effect of uneven lamination, regional coefficients which are made in both vertical and horizontal directions are searched automatically to solve this problem.

B. Filtering

In practical environment internal and external noise, to some extent, are unavoidably contained in image. It may result in obscure images or blurred features. In order to eliminate the noise effect, meanwhile, to keep it from expanding and save the details of image edge, a nonlinear filter algorithm is proposed in this paper.

Nonlinear filtering method is defined as two steps which are concluded as following:

Firstly, calculate of the sum V of the variances over the neighborhood.

$$V = \sum f^2[i,j] - \left(\sum f[i,j]\right)^2 / N \tag{5}$$

Suppose that f(i , j) is a gray value of point (i , j) in a image. V_1, V_2, V_3 and V_4 denotes neighborhoods' average gray values in the regions taking point (i , j) as the top left corner, the bottom left corner, the top right corner and the bottom right corner. Meanwhile, N denotes the number of the pixels in the region.

Secondly, choose the minimum of the values V_1, V_2, V_3 and V_4, as V_m, then, calculate the average gray value F(x , y) in the region of V_m.

In this context, noise reduction can be achieved effectively with a filter whose basic function is to compute the average gray levels in the region in which the value V_m is located. That is to say gray level of the point [i , j] is replaced by the means of gray levels of all points in the region where the value V_m is located.

$$F(i,j) = \sum f(i,j) / N \tag{6}$$

F(x, y) is as transformation gray value

C. Rough Edge Detection

There are many algorithms [7, 8] in edge detection, such as Roberts operator, Sobel operator, Prewitt operator, Lapcian operator and LOG operator. Different method has different characteristic. Take the Roberts operator for example, it is an approximation to the continuous gradient at that point and not at the point (i ,j) as might be accepted.

Fig. 2 A part's image

Sobel operator [8] is one of the pixel-level edge detection arithmetic. It detects the edge through convolution between image value of gray function f (i, j) and Sobel masks shown in Figure 3. It finds edge by calculating partial derivatives in 3×3 neighborhood. In our application Sobel edge detection is selected. The reason of using Sobel operator is that it is insensitive to noise and it has relatively small masks than other operator such as Robert operator, two-order Laplacian operator and so on. The measured part is put in the same position where the standard one is in procedure of calibration of camera. For example, in an image shown as figure 2, there are two distinguished grey value changes for measured part. The pixels are taken as the edge if they have maximum value of gray gradient.

Based on Sobel method derivative S_x in x and S_y in y directions are given as:

$$S_x = [f(i+1,j-1) + 2f(i+1,j) + f(i+1,j+1)] - [f(i-1,j-1) + 2f(i-1,j) + f(i-1,j+1)] \tag{7}$$

$$S_y = [f(i-1,j-1) + 2f(i,j-1) + f(i+1,j-1)] - [f(i-1,j+1) + 2f(i,j+1) + f(i+1,j+1)] \tag{8}$$

The gradient of each pixel is calculated according to $g(x,y) = \sqrt{(x^2 + y^2)}$.

Given a threshold value TH, if g(x , y) > TH, this point is regarded as an edge point. If $S_x > TH$ or $S_x < -TH$, pixel (i , j) is the location which attaches to the vertical edge; If $S_y > TH$ or $S_y < -TH$, pixel (i , j) is the location which attaches to the horizontal edge.

Through the process above, the edge location based on pixel level is found. And we assume that the edge pass though the centre of that pixel which we located before.

D. Subdivision Technology

The measurement of integral pixel can't generally satisfy requirement for the precision in industry measurement due to most available CCD digital cameras are megapixel in the market. These cameras usually applied CCD array covering a square of more than 100*100mm^2. Take one megapixel area CCD camera making an image in the square field of 100*100 mm^2 as an example, if rows and columns of CCD array are 1000 separately, and resolution of a integral pixel is 0.1 mm, which can't satisfy the requirement for the precision of industrial measurement. The method to raise resolution is to add pixel number of CCD array, while pixel needs a 4-time bigger in number to increase its resolution from 0.1 mm to 0.05 mm.

If the resolution of a field of 100*100 mm^2 is 0.01 mm, a area CCD camera with 100 megapixel is necessary, however, such camera is not available due to highest requirement of manufacturing technology. Therefore, it is impossible to achieve high-precision target only by increasing pixels of CCD array. Moreover, precision requirements for industrial parts measurement can't be met unless pixel is divided by means of software (subdivision Technology).

Extraction of sub-pixel edge is to identify edge accurate position within one pixel. The position is found through identifying the vertical distance between edge line and the centre of pixel and angle between edge line to CCD array border. The method is discussed in detail in this section.

1) Spatial Moments

The edge can be found accurately by means of sub-division technology [9-14], that is, through locating the vertical dimension l between the edge and the centre of pixel as well as the angle θ.

A continuous ideal edge model is shown in Figure 3. And it is characterized by four parameters h, k, l and θ. The edge is a straight line which separates two regions of constant gray values. The lower level has height h and the upper level is k higher than the lower level. The angle which the edge makes with the y axis is θ and l is the distance from the centre of the region to the edge.

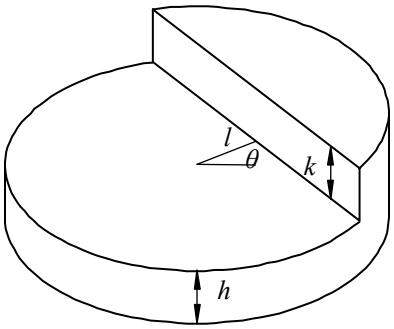

Fig. 3 Ideal continuous step edge model used for moment-based edge operator. There are two grey levels, h and $h+k$. The edge translation is l and orientation θ

The moments of a continuous image f (x , y) of order $p+q$ are defined by

$$M_{pq} = \iint x^p y^q f(x,y)dxdy \tag{9}$$

Let (x, y) denotes the centre of the moments, p is index of x and q stands for index of y. Since the region of integration is a disk with a radius of one, the limits of integration region is a unit circle, ie. $\sqrt{x^2+y^2} \le 1$.

A moment set of order n consists of all moments of order n and lower and is closed with respect to the operations such as rotation, translation, and scale transformation. For detecting edge point, only the moment set of order 2 is considered and computed. The moment set can be described as (M_{00} , M_{01} , M_{10} , M_{11} , M_{02} , M_{20}).

Without losing generality, let rotate of the disk by an angle θ, and the moment set is changed as specified by (M'_{00} , M'_{01} , M'_{10} , M'_{11} , M'_{02} , M'_{20}).

$$M'_{00} = M_{00} \tag{10}$$

$$M'_{10} = \cos\theta M_{10} + \sin\theta M_{01} \tag{11}$$

$$M'_{01} = -\sin\theta M_{10} + \cos\theta M_{01} \tag{12}$$

$$\begin{aligned} M'_{11} &= -\sin\theta\cos\theta M_{20} + \sin\theta\cos\theta M_{02} \\ &\quad + (\cos^2\theta - \sin^2\theta)M_{11} \end{aligned} \tag{13}$$

$$\begin{aligned} M'_{20} &= \cos^2\theta M_{20} + \sin^2\theta M_{02} \\ &\quad + 2\cos\theta\sin\theta M_{11} \end{aligned} \tag{14}$$

$$\begin{aligned} M'_{02} &= \sin^2\theta M_{20} + \cos^2\theta M_{02} \\ &\quad - 2\sin\theta\cos\theta M_{11} \end{aligned} \tag{15}$$

In order to work out l and θ, let rotate the edge region to align with the y axis as shown in Figure 4. At this position there is symmetry about the x axis, therefore

$$M'_{01} = 0 \tag{16}$$

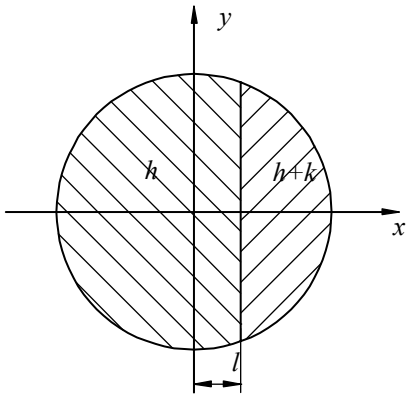

Fig. 4 Ideal edge aligned with the y-axis

Based on Equation (12) and Equation (16), θ is determined by Equation (17) as following:

$$\theta = \arctan\frac{M_{01}}{M_{10}} \tag{17}$$

Where

$$\begin{aligned} M'_{00} &= \int_{-1}^{1}\int_{-\sqrt{1-x^2}}^{\sqrt{1-x^2}} h dxdy + \int_{l}^{1}\int_{-\sqrt{1-x^2}}^{\sqrt{1-x^2}} k dxdy \\ &= h\pi + \frac{k\pi}{2} - k\sin^{-1} l - kl\sqrt{1-l^2} \end{aligned} \tag{18}$$

$$\begin{aligned} M'_{10} &= h\int_{-1}^{1}\int_{-\sqrt{1-x^2}}^{\sqrt{1-x}} x dxdy + k\int_{l}^{1}\int_{-\sqrt{1-x^2}}^{\sqrt{1-x}} x dxdy \\ &= k\cdot\frac{2}{3}(1-l^2)^{\frac{3}{2}} \end{aligned} \tag{19}$$

$$\begin{aligned} M'_{20} &= h\int_{-1}^{1}\int_{-\sqrt{1-x^2}}^{\sqrt{1-x^2}} x^2 dydx + k\int_{l}^{1}\int_{-\sqrt{1-x^2}}^{\sqrt{1-x^2}} x^2 dydx \\ &= 4h\int_{0}^{1} x^2\sqrt{1-x^2}dx + 2k\int_{l}^{1} x^2\sqrt{1-x^2}dx \end{aligned} \tag{20}$$

$$\int x^2\sqrt{1-x^2}d_x = \frac{1}{8}[x^3\sqrt{1-x^2} + \sin^{-1}x] + c \tag{21}$$

From Equation (20) and Equation (21) M'_{20} is determined

$$\begin{aligned} M'_{20} &= \frac{h\pi}{4} + \frac{k\pi}{8} + \frac{k}{2}l(1-l^2)^{\frac{3}{2}} \\ &\quad - \frac{k}{4}l\sqrt{1-l^2} - \frac{k}{4}\sin^{-1} l \end{aligned} \tag{22}$$

$$\begin{aligned} 4M'_{20} &= h\pi + \frac{k\pi}{2} + 2kl(1-l^2)^{\frac{3}{2}} \\ &\quad - kl\sqrt{1-l^2} - k\sin^{-1} l \end{aligned} \tag{23}$$

$$4M'_{20} - M'_{00} = 2kl(1-l^2)^{\frac{3}{2}} \tag{24}$$

Equation (19) and Equation (24) may now be combined to solve for *l*.

$$l = \frac{4M'_{20} - M'_{00}}{3M'_{10}} \tag{25}$$

Therefore, *l* and θ can be calculated by equation (17) and equation (25) respectively according to moment set of order 2.

2) Estimation of Moment Set

The moment set of order 2 can be estimated by correlating the elements in a 5x5 window mask as shown in Figure 5. Equations (26) (27) (28) (29) (30) and (31) given their definitions clearly.

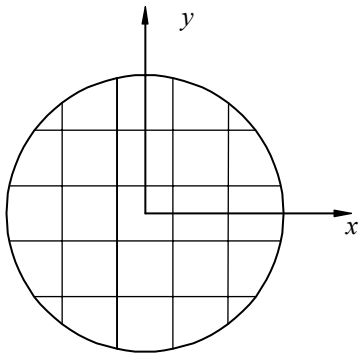

Fig. 5 The integral region within a radius of one is divided into 25 parts by a rectilinear grid whose space between is 0.4.

$$m_{00} = \iint d_x d_y \tag{26}$$

$$m_{10} = \iint x d_x d_y \tag{27}$$

$$m_{01} = \iint y d_x d_y \tag{28}$$

$$m_{11} = \iint xy d_x d_y \tag{29}$$

$$m_{20} = \iint x^2 d_x d_y \tag{30}$$

$$m_{02} = \iint y^2 d_x d_y \tag{31}$$

Each mask represents the value resulting from the integral of Equations (26) (27) (28) (29) (30) and (31). Each value is calculated by integral on the region shown in Figure 5. The details of these six masks are shown in Table Ⅰ, Table Ⅱ, Table Ⅲ, Table Ⅳ, Table Ⅴ and Table Ⅵ individually at bottom of this paper.

Put the centre of the integral pixel located at the edge on the position of the mask centre. Then 25 products can be obtained by multiplying the gray of 25 pixels and the corresponding value of m_{00} mask. And then the sum of 25 products is equal to M_{00}. Meanwhile, M_{01}, M_{10}, M_{11}, M_{02}, M_{20} can be obtained by the same way.

Once the moment set is obtained, the sub-pixel leveled location of edge point can be known as a result.

E. Extraction of sub-pixel edge

In this section, the algorithm of how to obtain sub-pixel leveled edge point is extraced as following steps:

Step 1, θ can be determined by M_{01} and M_{10} from Equation (17);

Step 2, from Equations (10) (11) and (14) M'_{00}, M'_{10} and M'_{20} can be determined;

Step 3, *l* can be determined from Equation (25).

Eventually the sub-pixel leveled edge can be found accurately through locating the vertical dimension between the edge and the centre of pixel as well as the angle θ.

The edge pass through an integral pixel, the gray values of the integral pixel and its neighborhood pixels is shown in Table VII.

TABLE VII. The gray values of the integral pixel and its neighborhood pixels

23	36	252	253	253
25	43	223	221	223
34	49	211	212	213
35	46	207	210	209
33	35	207	210	211

Given the information as shown in Table VII, we first put the centre of the integral pixel located at the edge on the position of the m_{00} mask centre shown in Table 1. Then 25 products can be obtained by multiplying the gray of 25 pixels and the corresponding value of m_{00} mask. And then the sum of 25 products is equal to M_{00}.

$$M_{00} = 476.2624$$

Meanwhile, $M_{01}, M_{10}, M_{11}, M_{02}, M_{20}$ can be obtained by the same way.

$$M_{10} = 113.8387$$
$$M_{01} = 11.9377$$
$$M_{11} = 4.4332$$
$$M_{20} = 97.6854.$$
$$M_{02} = 126.1745$$

So, from Equation (17) θ is determined.

$$\theta = 5.98^\circ.$$

Secondly, from Equations (10) (11) and (14) M'_{00}, M'_{10} and M'_{20} can be obtained as following:

$$M'_{00} = 476.2624$$
$$M'_{10} = 114.4691$$
$$M'_{20} = 125.6565.$$

Thirdly, l can be calculated by Equation (21), $l = 0.07677$.

So the edge at subpixel level can be located accurately by the algorithms above as shown in Figure 6.

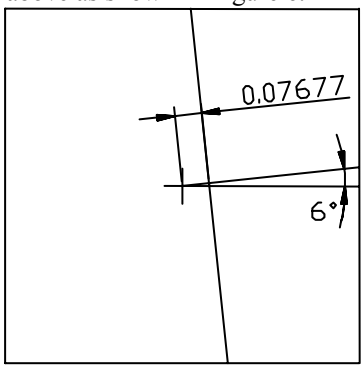

Fig. 6 The subpixel leveled edge location

III. Experimental Setup and Result

A. Experimental Setup

The method introduced in sections above is implemented online by using system as shown in Figure 7.

Fig. 7 Experimental machine of the measurement

A brief introduction of this system is given as following. Four parts are included in this system: illumination system, digital camera system, mechanism system and software system. Illumination system provides an optical background for digital camera (dark objects on a light background or light objects on a dark background) in order to make the edge of parts' image stand in vivid contrast against the background. CCD camera captures image of object which is processed later. Computer runs image processing software and give measure results. Comprising of manipulator and conveying machines mechanism system is used to load and deliver parts.

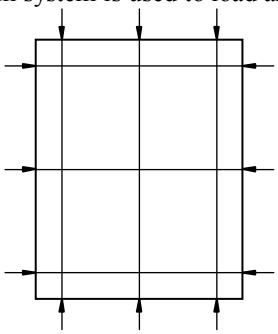

Fig. 8 Six dimensions of workpiece to be measured

The method described above is implemented to sort workpiece which is a rectangular ceramic piece sized of 60mm*50mm*0.4mm. Due to the manufacturing process the products are distributed in range between 0.1 mm and 0.2 mm. There are needs to measure and classify the products to 15 kinds according to its sides. Six dimensions need to be measured, as the Figure 8 shown.

According to the theory of edge detection and subdivision technology, the dimension of standard part is L_s and two endpoints' coordinates of line to be measured are (X_1 , Y_1) and (X_2 , Y_2); the dimension of part to be measured is L_m, and the coordinates are (x_1 , y_1) and (x_2 , y_2). Then L_m can be expressed by Equation (32).

$$L_m = \frac{\sqrt{(x_2 - x_1)^2 + (y_2 - y_1)^2}}{\sqrt{(X_2 - X_1)^2 + (Y_2 - Y_1)^2}} L_s \qquad (32)$$

B. Experimental Results

In the process of using method of calibration of camera for measurement every time, standard parts are first measured, and then other parts. Standard and other parts should be in the same position so that they can reduce impact on measurement precision resulting from drawbacks of camera lens and change of optical background.

Online experimental results shown in Figure 9 and Figure 10 respectivelly, where L_{11}, L_{12}, L_{13}, W_{11}, W_{12}, W_{13} denote the six dimensions in the first measuring, L_{21}, L_{22}, L_{23}, W_{21}, W_{22}, W_{23} denote the six dimensions in the second measuring and L_{31}, L_{32}, L_{33}, W_{31}, W_{32}, W_{33} denote the six dimensions in the third measuring. From the results we can see that the maximum bias is within 0.01 mm. The results demonstrates that sub-pixel technology applied in measurement of calibration of camera can raise resolution of integral pixel from 0.1 mm to 0.005 mm; meanwhile, precision being 1/20 of resolution of integral pixel.

IV. Conclusion and Discussion

With the help of CCD digital camera, image collecting card and computer technology, it has theoretical and technological possibility to implement high accurate and non-touch measurement in several industrial applications. Calibration of camera, filtering, edge detection, the spatial moment and the subdivision technology are combined to help improve the measure precision. The application in industry further demonstrates our proposed method is a new non-contact, high accuracy, non-wear and efficient method. Especially, this method gives superior performance compared with other known method to measurement of volume-produced industrial manufacture. Hence, high accuracy measure method based on subpixel technology, whose theory and technology can be applied to practical application, will have a bright future in industrial measurement.

References

[1] Wu Lisheng, Yang Lifeng, Li Yuanzong. “Effect of alignment error to measurement accuracy in CCD dimension,” Measuring System Chinese Journal of Scientific Instrument. J. Chinese, vol. 10, pp. 1093-1096, 1100, 2005.

[2] Wang Zhu, Tong Xiajun. “Measured paper money size,” Electronic Measurement Technology. J. Chinese, vol. 4, pp. 22-23, 2005.

[3] Liu Qingming, Wang Longshan, Chen Xiangwei, Cui Zhi. “Image measurement on internal thread of ball screws,” China Mechanical Engineering. J. Chinese, vol. 5, pp. 1328-1331, 2005.

[4] Yang Lifeng. “Application of machine vision in autosort system of sheet,” Mechanical Engineering& Automation. J. Chinese, vol. 3, pp. 18-19, 21, 2004.

[5] Yang Lifeng, Han Jiwan, Li yuanzong. “Application of high resolution measurement technique with area CCD,” Journal of Taiyuan University of Technology. J. Chinese, vol. 5, pp. 455-458, 2001.

[6] Zheng Lihong, Li Yuanzong, Yang Lifeng. “Application of subdivision technology in industrial measurement,” T.D.WEN. ISTM/2003 5th International Symposium on Test and Measurement. C. Chinese, Beijing: International Academic Publishers World Publishing Corporation, pp. 2881-2882, 2003.

[7] K. R. Castleman. Digital image processing.

[8] I. Sobel. “Neighbourhood coding of binary images fast contour following and general array binary processing,” Computer Graphics and Image Processing. J. vol. 8, pp. 127–135, 1978.

[9] O’Gorman, Lawrence. “Sub-pixel precision of straight-edged shapes for rRegistration and measurement,” IEEE Transaction on Pattern Analysis and Machine Intelligence. J. vol. 18(7), pp. 746-751, 1996.

[10] Mitchell, O. Robert, Lyvers, Edward P, etc. “Recent results in precision measurements of edges, angles, areas and perimeters,” Proceedings of SPIE-The International Society for Optical Engineering. C. WA, USA: SPIE, 1987: 123-134.

[11] Li Hongjun, Han Jiwan. “Digital image processing and its application,” Computer Measurement & Control. J. Chinese, vol. 10, pp. 620-622, 2002.

[12] Yang Lifeng, Wu Lisheng, Liu Jianhong, Li Yuanzong. “Analysis of alignment error in dimension measuring system of machine vision,” Journal of Taiyuan University of Technology. J. Chinese, vol. 3, pp. 332-335, 2004.

[13] Liu Li, Shi Yinggang, Li Yuanzong. “Study on the edge detection and pixel subdivision algorithms in the graphical measurement,” Sci-Tech Information Development & Economy. J. Chinese, vol. 5, pp. 177-178, 2006.

[14] Yao Fenglin, Zhan Haiying, Li Yuanzong. “A survey of edge detection technology in computer vision,” Mechanical Engineering& Automation. J. Chinese, vol. 5, pp. 108-110, 2005.

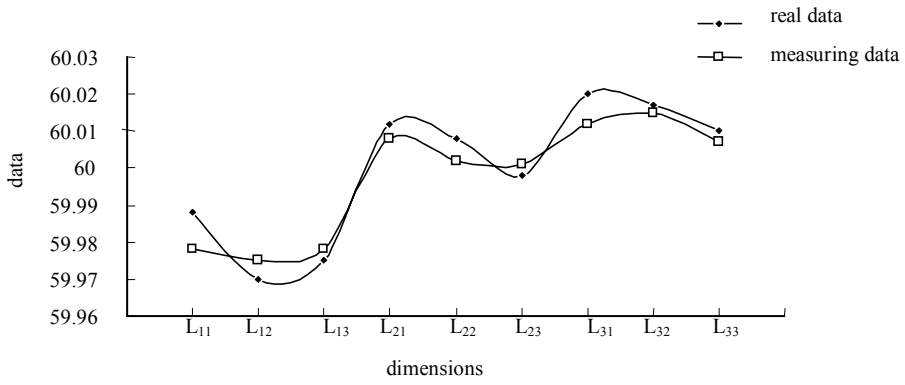

Fig. 9 Length dimensions measuring data

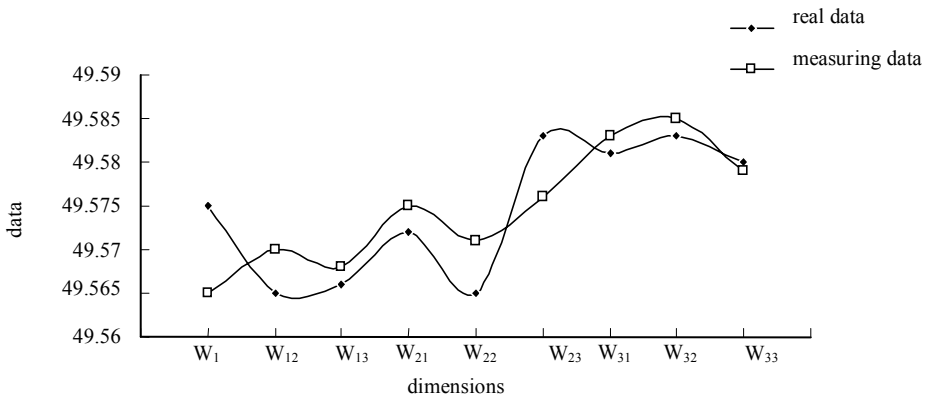

Fig. 10 Width dimensions measuring data

TABLE I. m_{00}mask

0.0219	0.1231	0.1573	0.1231	0.0219
0.1231	0.1600	0.1600	0.1600	0.1231
0.1573	0.1600	0.1600	0.1600	0.1573
0.1231	0.1600	0.1600	0.1600	0.1231
0.0219	0.1231	0.1573	0.1231	0.0219

TABLE II. m_{10}mask

-0.0147	-0.0469	0.0000	0.0469	0.0147
-0.0933	-0.0640	0.0000	0.0640	0.0933
-0.1253	-0.0640	0.0000	0.0640	0.1253
-0.0933	-0.0640	0.0000	0.0640	0.0933
-0.0147	-0.0469	0.0000	0.0469	0.0147

TABLE III. m_{01}mask

0.0147	0.0933	0.1253	0.0933	0.0147
0.0469	0.0640	0.0640	0.0640	0.0469
0.0000	0.0000	0.0000	0.0000	0.0000
-0.0469	-0.0640	-0.0640	-0.0640	-0.0469
-0.0147	-0.0933	-0.1253	-0.0933	-0.0147

TABLE IV. m_{11}mask

-0.0098	-0.0352	0.0000	0.0352	0.0098
-0.0352	-0.0256	0.0000	0.0256	0.0352
0.0000	0.0000	0.0000	0.0000	0.0000
0.0352	0.0256	0.0000	-0.0256	-0.0352
0.0098	0.0352	0.0000	-0.0352	-0.0098

TABLE V. m_{20}mask

0.0099	0.0194	0.0000	0.0194	0.0099
0.0719	0.0277	0.0000	0.0277	0.0719
0.1019	0.0277	0.0000	0.0277	0.1019
0.0719	0.0277	0.0000	0.0277	0.0719
0.0099	0.0194	0.0000	0.0194	0.0099

TABLE VI. m_{02}mask

0.0099	0.0719	0.1019	0.0719	0.0099
0.0194	0.0277	0.0277	0.0277	0.0194
0.0000	0.0000	0.0000	0.0000	0.0000
0.0194	0.0277	0.0277	0.0277	0.0194
0.0099	0.0719	0.1019	0.0719	0.0099